**Advances in Nano Research**, *Vol. 18, No. 4 (2025) 337-350*
https://doi.org/10.12989/anr.2025.18.4.337


# A pathway to sports innovation through the stability performance of lightweight functionally graded tubular structures

Donglin Xiao*[1], Mostafa Habibi[2,3,4], Belgacem Bouallegue[5] and Maryam Bagheri[6]

*[1]Sports College, Xi'an University of Petroleum, Xi'an 710065, Shaanxi, China*
*[2]Universidad UTE, Facultad de Arquitectura y Urbanismo, Calle Rumipamba S/N y Bourgeois, Quito, 170147, Ecuador*
*[3]Department of Biomaterials, Saveetha Dental College and Hospital, Saveetha Institute of Medical and Technical Sciences, Chennai, 600 077, India*
*[4]Institute of Research and Development, Duy Tan University, Da Nang, 550000, Viet Nam*
*[5]Department of Computer Engineering, College of Computer Science, King Khalid University, ABHA, 61421, Saudi Arabia*
*[6]Researcher, Hoonam Sanat Farnak, Engineering Company, Ilam, Iran*

(*Received December 23, 2022, Revised March 7, 2025, Accepted March 10, 2025*)

**Abstract.** Small-scale tubular structures have garnered considerable interest owing to their exceptional mechanical qualities, making them suitable for applications requiring lightweight and durable designs. This work examines the stability and buckling behavior of these structures via an integrated approach that merges beam theory with modified couple stress theory, yielding a more accurate comprehension of micro and nanoscale phenomena. The findings are particularly relevant to the sports industry, where advances in equipment and practices may considerably impact player performance and safety. This study looks at how these structures may improve the design of high-performance sports equipment, such as lightweight yet stable bicycle frames, ski poles, and gymnastic vaulting poles, by increasing their strength-to-weight ratio for better performance. The study emphasizes the potential applications in protective equipment and wearable technologies, where maintaining structural integrity is essential for ensuring longevity while preserving mobility. The comprehension of mechanical stability has progressed, leading to the development of a method for integrating advanced structural mechanics into sports engineering, thereby facilitating innovations that improve athletic performance and safety.

**Keywords:** athletic performance; buckling analysis; protective equipment design; small-scale structures; sports engineering

## 1. Introduction

There has been a significant increase in demand for lightweight and durable materials across a variety of industries, particularly sports engineering. The use of advanced materials in sports equipment has dramatically improved athletic performance and safety (Huo *et al*. 2021, Zhang *et al*. 2021, Guo *et al*. 2024, Li *et al*. 2024, Liang *et al*. 2024, Xiao *et al*. 2024, Zisong and Habibi 2024). Functionally graded materials (FGMs) are an important research domain due to their distinct properties (Omidi *et al*. 2013, Mousavi *et al*. 2017, Shahabinejad *et al*. 2018). Functionally graded materials are composites distinguished by gradual changes in composition and structure, which cause corresponding changes in mechanical properties throughout their volume (Panchal and Ponappa 2022). This gradation improves specific performance attributes such as strength, flexibility, and weight, and is tailored to a variety of applications. The use of functionally graded materials in athletic equipment has been transformative (Song *et al*. 2024, Wang *et al*. 2024b, Yin *et al*. 2024, Liu *et al*. 2025). The use of functionally graded materials in sports equipment has been revolutionary. In sports such as cycling, snowboarding, and skiing, lightweight constructions have been demonstrated to enhance speed and performance significantly. Materials like carbon fiber, which can be customized for particular applications, have played a crucial role in these developments (Wang *et al*. 2024a, c, 2025a). Designing equipment that combines lightweight properties with improved mechanical performance is essential for athletes seeking optimal results. The idea of functionally graded materials originated in Japan in 1984 as part of a space plane project, with the objective of creating materials that can endure significant temperature gradients (He *et al*. 2025, Zhao *et al*. 2025). Since then, FGMs have been utilized across multiple domains, such as aerospace, automotive, and biomedical engineering, owing to their customized properties. The integration of functionally graded materials in sports engineering has resulted in the creation of equipment that satisfies the mechanical requirements of high-performance sports while enhancing athlete safety by minimizing injury risk through superior material characteristics (Wang *et al*. 2022, Jia *et al*. 2023, Zhang *et al*. 2023a, b, c, Qi *et al*. 2024). The ongoing advancement of material science, especially regarding the development and utilization of functionally graded materials, presents considerable potential for the future of sports engineering. Engineers can utilize the distinct properties of these materials to design and produce sports equipment that enhances performance, durability, and safety, thus advancing athletic achievement (Mirjavadi *et al*.

*Corresponding author, Ph.D.,
E-mail: wyqtsh2009@163.com



ISSN: 2287-237X (Print), 2287-2388 (Online)

2020b, c, d, e).

Functionally graded materials have a wide range of technical applications, but their use in athletic equipment design is limited. Modern sports equipment is primarily made of uniform materials, which may not enhance performance as much as functionally graded materials (Zhang *et al*. 2020, Wang *et al*. 2024i). The limited use of FGMs stems from the difficulty of producing these materials with the complex geometries required for sporting equipment, as well as a lack of research on their specific applications in this domain (Wang *et al*. 2024f, Wu *et al*. 2024). Furthermore, while the mechanical properties of functionally graded materials have been extensively studied in a variety of engineering applications, there is a significant research gap in their stability and buckling behavior in small-scale tubular structures used in sports equipment (Leoni *et al*. 2023). Conventional buckling analysis methods frequently overlook size-dependent effects, which are critical at micro and nanoscale dimensions. The modified pair stress theory offers a framework for integrating small-scale effects, however, its application in evaluating the buckling behavior of FGM-based sports equipment remains underexplored (Wang *et al*. 2024b). Addressing these gaps is essential for the advancement of sports engineering. An in-depth analysis of the stability performance of light-weight, functionally graded tubular structures can facilitate the advancement of sports equipment that enhances athletic performance via optimized strength-to-weight ratios while also mitigating the risk of buckling failure (Gu *et al*. 2022). Consequently, there is a pressing requirement for research that integrates advanced material science with improved mechanical analysis to explore the potential of functionally graded materials in sports applications (Wang *et al*. 2024e, g, h, Zhang *et al*. 2024b, Zhu *et al*. 2024a, b, Xia *et al*. 2025).

The incorporation of functionally graded materials in the design of sports equipment is expected to greatly improve both athletic performance and safety. Functionally graded materials demonstrate a seamless transition in composition and structure, leading to customized mechanical properties that are finely tuned for particular applications. This distinctive feature facilitates the creation of equipment that optimizes strength, flexibility, and weight, enhancing performance and minimizing injury risk (Saad 2022). The utilization of functionally graded materials in sports engineering is significant. Lightweight constructions in sports such as cycling, snowboarding, and skiing significantly enhance speed and performance. Carbon fiber, tailored for particular applications, has greatly enhanced these developments (El-Galy *et al*. 2019). The ongoing advancements in material science, especially regarding the development and application of functionally graded materials, present considerable opportunities for the future of sports engineering. Engineers can utilize the distinct characteristics of these materials to design and produce sports equipment that enhances performance, durability, and safety, thereby facilitating athletic achievement.

This study investigates the stability and buckling properties of small-scale tubular structures made from functionally graded materials (FGMs) in the context of sports engineering. This study seeks to enhance understanding of the mechanical behavior of structures at micro and nano-scale levels through the integration of beam theory and modified couple stress theory (Dai *et al*. 2021, Shi *et al*. 2022, He *et al*. 2024, Man *et al*. 2024, Wang *et al*. 2024d, 2025b, Xue *et al*. 2024, Yu *et al*. 2024, Zhang *et al*. 2024c, Zhao *et al*. 2024, Zhiqiang *et al*. 2024, Jining *et al*. 2025, Zhou *et al*. 2025). This study examines several important facets:

• Material Characterization: This analysis will examine functionally graded materials, focusing on their composition, microstructure, and the impact of these factors on mechanical properties, including strength, flexibility, and weight distribution. This characterization is crucial for customizing materials to fulfill the specific requirements of sports equipment (Nayak and Armani 2022).

• Theoretical Framework Development: This research seeks to establish a theoretical framework integrating beam theory and modified couple stress theory. This approach seeks to provide a more precise depiction of the mechanical behavior of small-scale structures, considering size-dependent effects frequently neglected in conventional analyses (Partskhaladze *et al*. 2019).

• Buckling Analysis: A thorough buckling analysis of small-scale tubular structures will be performed to determine their stability under a variety of loading conditions. This analysis is critical for determining the structural integrity of sports equipment components that experience dynamic forces during use, such as bicycle frames, ski poles, and gymnastic vaulting poles (Godat *et al*. 2012).

• Application to Sports Equipment Design: The results from the theoretical and analytical studies will guide the creation of high-performance sports equipment. The goal is to improve the strength-to-weight ratio of these products, which will lead to better performance and safety for athletes. This application is especially relevant for creating lightweight and stable components that can endure the challenging requirements of different sports (Lin and Qiyuan 2023).

This study aims to connect advanced material science with practical applications in sports engineering, ultimately fostering the creation of innovative equipment designed to improve athletic performance and ensure safety (Yan *et al*. 2024). Despite advancements in the application of functionally graded materials across various engineering domains, notable gaps persist in their use for sports equipment design, especially concerning the analysis of small-scale, non-uniform tubular structures subjected to complex loading conditions (Chen *et al*. 2022, Li *et al*. 2025a). Many current studies concentrate on uniform geometries, overlooking the combined impacts of nonlocal elasticity, material gradation, and cross-sectional variability, which are essential for accurately predicting the stability and buckling performance of sports equipment (Wei *et al*. 2024, Li *et al*. 2025b). The literature has not sufficiently addressed the influence of boundary conditions and size-dependent phenomena at the nanoscale. The identified shortcomings impede a thorough understanding and optimization of FGMs for advanced sports applications

(Gao *et al*. 2025, Wang *et al*. 2025c). This study introduces a mathematical framework to analyze the stability behavior of non-uniform, porosity-dependent functionally graded tubular structures. This study combines advanced shear deformation theory, nonlocal strain gradient theory, and the Hamilton principle to accurately address important size-dependent effects and sensitivities related to boundary conditions. The use of varied cross-sectional profiles, illustrated by four unique mathematical functions, marks a significant advancement in simulating realistic designs for sports equipment. This research stands out because of its diverse approach to the intricate relationships between geometry, material gradation, and size effects, providing a thorough stability analysis of functionally graded materials in sports engineering. The results offer valuable perspectives on creating lightweight, high-performance sports gear, emphasizing enhanced mechanical stability and safety under various loading scenarios. This research lays the groundwork for developing new materials and structures aimed at improving athletic performance and ensuring safety.

Fig. 1 Non-uniform tubular structures in sports such as, bicycle frames, ski poles, and gymnastic vaulting poles, optimized for strength, weight, and performance

## 2. Mathematical modeling

To maximize performance and safety, modern sports equipment should be made of lightweight, strong, and highly stable materials. The use of porosity-dependent non-uniform functionally graded microtubes is an innovative solution to this issue. These structures are particularly useful in applications requiring weight reduction, increased strength, and dynamic stability for athletic performance, such as bicycle frames, ski poles, and gymnastics vaulting poles. This section provides a thorough mathematical and mechanical analysis of the buckling behavior of non-uniform FGM microtubes, as well as recommendations for improving their design to meet the stringent requirements of sports engineering (Mirjavadi *et al*. 2020a, 2022a, c, Kazemi *et al*. 2023).

### *2.1 Geometric configuration*

To achieve a balance between strength and weight distribution in sports applications, the non-uniform geometry of tubular components is often a carefully considered design decision. For example (Fig. 1):

• Bicycle frames: To reduce weight while retaining structural integrity, tubes are thinner in straight sections and thicker at joints.

• Ski poles: Gradual tapering increases strength and aerodynamic efficiency in areas with concentrated forces, such as the handle and tip of ski poles.

• Gymnastic vaulting poles: Gymnastic vaulting poles of varying thicknesses aid in stress distribution during dynamic bending.

Weight and stiffness can be optimized along the length of the microtube by modeling it with an axial length '$L$', an outer radius '$Ro(x)$', and a thickness '$t$' that are functions of the axial coordinate '$x$' (Fig. 2).

Suppose a uniform internal radius, '$R_{in} = D_{in}/2$', so the thickness is calculated as follows:

$$t(x) = Ro(x) - R_{in} \tag{1a}$$

where '$Ro(x)$' is the external radius function. Also, the three types of nonuniform functions involving the linear, concave, and convex types are supposed for the external radius tube to make the nonuniformity, which is figured in Fig. 2, and the mathematical formulation of them is represented in the following (Xia *et al*. 2025).

Nonuniform external linear function:

$$Ro(x) = \frac{1253}{957}\left(1 - \frac{1}{2}\frac{x}{L}\right) R_{initial} \tag{1b}$$

Nonuniform external concave function:

$$Ro(x) = \frac{1211}{908}\left(1 - \frac{183}{625}\frac{x}{L}\right)^2 R_{initial} \tag{1c}$$

Nonuniform external convex function:

$$Ro(x) = \frac{191}{151}\left(1 - \frac{3}{4}\frac{x}{L}\right)^{0.5} R_{initial} \tag{1d}$$

where '$R_{initial}$' is the external radius at '$x = 0$'. Also, for the external uniform radius, '$Ro(x) = R_{initial}$'.

### *2.2 Material gradation for enhanced performance*

The use of functionally graded materials (FGMs) with porosity provides a transformative approach to optimizing sports equipment in which both lightweight properties and structural stability are required. FGMs' material properties vary gradually throughout the structure, allowing for tailored mechanical responses that improve performance, durability, and athlete safety (Afshari Behzad *et al*. 2022, Mirjavadi *et al*. 2022b, 2023, Kazemi *et al*. 2024).

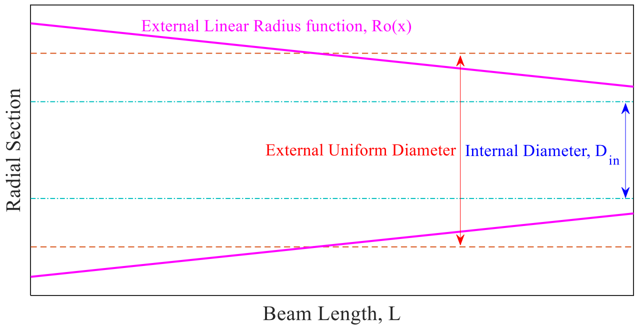


(a) Nonuniform linear Section

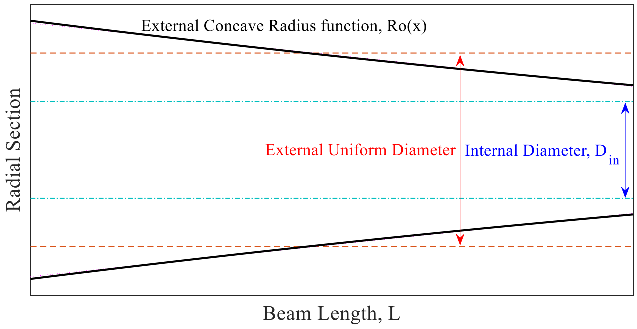


(b) Nonuniform Concave Section

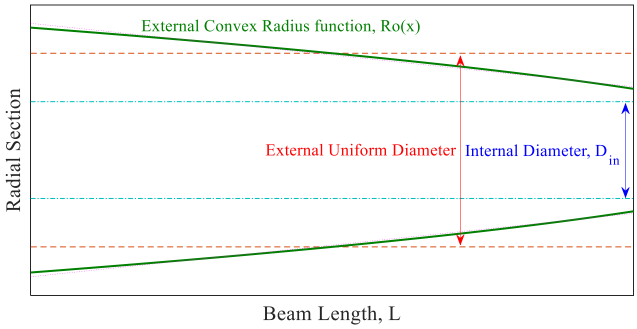


(c) Nonuniform Convex Section

Fig. 2 A tube section schematic involves three types of non-uniform sections: nonuniform concave, linear, and convex

### *2.2.1 Porosity effects on lightweight design and stability*

Porosity in FGMs significantly reduces weight, which is critical in sports applications that require high speed, agility, and energy efficiency. By strategically incorporating graded porosity, the material's density can be optimized to maintain strength while removing unnecessary mass.

• Cycling: Using a lightweight bicycle frame with porosity-graded materials improves acceleration and reduces fatigue during long rides, thereby increasing endurance.

• Skiing: Ski poles with optimized porosity improve maneuverability while maintaining strength in high-stress areas, resulting in greater skier control.

• Gymnastics: A vaulting pole with precise porosity levels increases flexibility and energy absorption, preventing failure under dynamic loads.

Although these advantages are significant, uncontrolled porosity can reduce stiffness and stability, particularly in load-bearing sports equipment. Excessive porosity can reduce buckling resistance, making the structure more prone to deformation when exposed to external forces. As a result, striking the right balance between weight reduction and mechanical integrity is critical to ensuring both performance and safety.

### *2.2.2 Non-uniform material distribution for sports optimization*

In non-uniform tubular structures, such as bicycle frames, ski poles, and gymnastic vaulting poles, functionally graded porosity allows for:

• Weight reduction in low-stress regions to enhance speed and ease of movement.

• Higher density in critical load-bearing areas to prevent instability and premature buckling.

• Gradual stiffness variation to absorb impact forces, thereby increasing resilience and durability.

Sports engineers can use advanced porosity-dependent material gradation to design equipment that improves athletic performance while ensuring long-term reliability. This approach represents a significant advancement in sports engineering, allowing for the creation of lighter, stronger, and more efficient sports structures.

### *2.2.3 Functionally graded materials*

Functionally graded materials are important in sports applications because they provide a smooth transition in mechanical properties. The gradation can be customized to meet specific needs:

• Strength-to-Weight Ratio: Gradation increases stiffness in high-stress regions while decreasing weight in low-stress areas.

• Impact Resistance: Gradual material transitions increase energy absorption, lowering the likelihood of catastrophic failure during high-impact activities.

• Fatigue Resistance: Non-uniform FGMs distribute stresses more evenly, allowing sports equipment to last longer under repeated loading.

Porosity-dependent material properties, such as Young's modulus ($E$), are defined as functions of both radial and axial positions:

$$E(x,r) = \beta(E_{in} - E_{out})\left(\frac{r - R_{in}}{t(x)}\right)^{fgm} cos\left(\frac{\pi}{2}\frac{r - R_{in}}{t(x)}\right) + E_{in} + (E_{out} - E_{in})\left(\frac{r - R_{in}}{t(x)}\right)^{fgm} - E_{in}\beta\, cos\left(\frac{\pi}{2}\frac{r - R_{in}}{t(x)}\right) \tag{2a}$$

where '$fgm$' is the FGM parameter, '$\beta$' is the porosity parameter, '$E_{in}$' is the Elastic modulus in the internal surface ($r = R_{in}$), and '$E_{out}$' is the Elastic modulus at the external surface ($r = R_o$). Also, the Poison ratio ($\nu$) is defined as follows:

$$\nu(x,r) = \beta(\nu_{in} - \nu_{out})\left(\frac{r - R_{in}}{t(x)}\right)^{fgm} cos\left(\frac{\pi}{2}\frac{r - R_{in}}{t(x)}\right) + \nu_{in} + (\nu_{out} - \nu_{in})\left(\frac{r - R_{in}}{t(x)}\right)^{fgm} - \nu_{in}\beta\, cos\left(\frac{\pi}{2}\frac{r - R_{in}}{t(x)}\right) \tag{2b}$$

where, Poison ratio at the internal and external surface are '$\nu_{in}$' and '$\nu_{out}$'.

### 2.3 Governing equations

The analysis uses the Timoshenko beam theory to account for shear deformation and rotational inertia and the modified couple stress theory to account for size-dependent effects important in small-scale structures to generate the governing equations for the buckling analysis for the porosity-dependent nonuniform FGM tube. Using the energy principle based on the conservation of energy method, the total energy in the system is composed of potential strain energy, strain energy ($U$), and potential energy due to the external work ($V$) performed by applied forces. For buckling analysis, the total potential energy of the system is given as:

$$\Pi = U - V = 0 \tag{3a}$$

Since the system is in equilibrium at the buckling point, the variation of total energy must be zero, i.e.,

$$\delta U - \delta V = 0 \tag{3b}$$

The virtual potential energy due to the axial buckling force '$F$' is calculated as follows:

$$\delta V = \frac{1}{2}\delta\left(\iiint F\left(\frac{\partial w}{\partial x}\right)^2 dv\right) \tag{3c}$$

Also, the virtual strain energy ($\delta V$) is calculated as follows:

$$\delta U = \frac{1}{2}\delta\left(\iiint (\varepsilon_{ij}{:}\,\sigma_{ij} + m_{ij}{:}\,\chi_{ij})dv\right) \tag{3d}$$

where '$\varepsilon$', '$\sigma$', '$\chi$', and '$m$' are the strain, stress, symmetric curvature, and modified stress tensors, respectively. The strain tensors are calculated as follows:

$$\varepsilon_{ij} = \frac{1}{2}\left(\bar{u}_{i,j} + \bar{u}_{j,i}\right) \tag{4}$$

where '$\bar{u}$' is the displacement field according to the Timoshenko beam theory and they consider as follows:

$$\bar{u} = (u_x)_i + \left(u_y\right)_j + (u_z)_k \tag{5a}$$

$$u_x = u(x) - z\varphi(x) \tag{5b}$$

$$u_y = 0 \tag{5c}$$

$$u_z = w(x) \tag{5d}$$

where '$u$', '$w$', and '$\varphi$' are the axial, lateral and rotational component, respectively. According to first-order shear deformation displacement fields, the strain tensors ($\varepsilon_{ij}$) are calculated as follows:

$$\varepsilon_{xx} = \frac{\partial u}{\partial x} + z\left(\frac{\partial \varphi}{\partial x}\right) \tag{6a}$$

$$\varepsilon_{xz} = \varepsilon_{zx} = \frac{1}{2}\varphi + \frac{1}{2}\frac{\partial w}{\partial x} \tag{6b}$$

$$\varepsilon_{xy} = \varepsilon_{yx} = \varepsilon_{yy} = \varepsilon_{yz} = \varepsilon_{zy} = \varepsilon_{zz} = 0 \tag{6c}$$

Then the stress tensors ($\sigma_{ij}$) are calculated as follows:

$$\sigma_{xx} = E\frac{\partial u}{\partial x} + Ez\left(\frac{\partial \varphi}{\partial x}\right) \tag{7a}$$

$$\sigma_{xz} = \sigma_{zx} = \frac{1}{2}GK_S\varphi + \frac{1}{2}GK_S\frac{\partial w}{\partial x} \tag{7b}$$

$$\sigma_{xy} = \sigma_{yx} = \sigma_{yy} = \sigma_{yz} = \sigma_{zy} = \sigma_{zz} = 0 \tag{7c}$$

where '$G(x,r) = E(x,r)/(2+2\nu)$', and '$K_S$' is shear correction factor and it calculated as follows (Wang *et al.* 2024b):

$$K_S = \frac{K_1}{K_2} \tag{7d}$$

$$K_1 = 6(1+\vartheta(x)^2)^2\left(1+\vartheta(x)\right)^2 \tag{7e}$$

$$\vartheta(x) = \frac{R_{in}}{R_o(x)} \tag{7f}$$

$$\begin{aligned} K_2 = {} & (7 + 14\vartheta(x) + 8\vartheta(x)^2)(1+\vartheta(x)^2)^2 \\ & + 4\vartheta(x)^2(5 + 10\vartheta(x) + 4\vartheta(x)^2) \end{aligned} \tag{7g}$$

Also, the symmetric curvature tensors ($\chi_{ij}$) are calculated as follows:

$$\chi_{xy} = \chi_{yx} = \frac{1}{4}\frac{\partial \varphi}{\partial x} - \frac{1}{4}\frac{\partial^2 w}{\partial x^2} \tag{8a}$$

$$\chi_{xx} = \chi_{xz} = \chi_{yy} = \chi_{yz} = \chi_{zx} = \chi_{zy} = \chi_{zz} = 0 \tag{8b}$$

Then the modified couple stress tensors ($m_{ij}$) are calculated as follows:

$$m_{xy} = m_{yx} = \frac{1}{2}GK_S\frac{\partial \varphi}{\partial x}l^2 - \frac{1}{2}GK_S\frac{\partial^2 w}{\partial x^2}l^2 \tag{9a}$$

$$m_{xx} = m_{xz} = m_{yy} = m_{yz} = m_{zx} = m_{zy} = m_{zz} = 0 \tag{9b}$$

The strain energy ($U$) is calculated by combining Eqs. (6)-(9) with Eq. (3b). Using the energy conservation method, the governing equations and boundary conditions for the buckling stability of the porosity-dependent nonuniform FGM tube are determined.

*'$\delta u$'*

$$-\frac{\partial}{\partial x}\left(\Theta_8\frac{\partial u}{\partial x}\right) = 0 \tag{10a}$$

*'$\delta w$'*

$$\begin{aligned} & \frac{\partial^2}{\partial x^2}\left(\Theta_{14}\left(\frac{\partial \varphi}{\partial x} + \frac{\partial^2 w}{\partial x^2}\right)\right) + \frac{\partial^2}{\partial x^2}\left(\Theta_{14}\left(\frac{\partial^2 w}{\partial x^2}\right)\right) \\ & -\frac{1}{2}\frac{\partial}{\partial x}\left(\Theta_8\left(\varphi + \frac{\partial w}{\partial x}\right)\right) - \frac{1}{4}l^2\frac{\partial}{\partial x}\left(\Theta_8\left(\varphi + \frac{\partial w}{\partial x}\right)\right) \\ & -\frac{\partial^2}{\partial x^2}\left(\Theta_{14}\left(\frac{\partial \varphi}{\partial x} + \frac{\partial^2 w}{\partial x^2}\right)\right) + l^2\frac{\partial^2}{\partial x^2}\left(\Theta_{16}\left(\frac{\partial^2 w}{\partial x^2}\right)\right) \end{aligned} \tag{10b}$$

$$+\frac{3}{8}l^2\frac{\partial^2}{\partial x^2}\left(\Theta_8\left(\frac{\partial\varphi}{\partial x}+\frac{\partial^2 w}{\partial x^2}\right)\right)$$
$$-\frac{1}{2}l^2\frac{\partial^2}{\partial x^2}\left(\Theta_{16}\left(\frac{\partial^2 w}{\partial x^2}\right)\right)$$
$$-\frac{1}{2}l^2\frac{\partial^2}{\partial x^2}\left(\Theta_{16}\left(\frac{\partial\varphi}{\partial x}+\frac{\partial^2 w}{\partial x^2}\right)\right)$$
$$-\frac{\partial^2}{\partial x^2}\left(\Theta_{14}\left(\frac{\partial^2 w}{\partial x^2}\right)\right)-\frac{\partial}{\partial x}\left(F\frac{\partial w}{\partial x}\right)=0$$

'$\delta\varphi$'

$$+\frac{1}{2}\Theta_8\left(\frac{\partial w}{\partial x}\right)+\frac{1}{4}l^2\Theta_8\left(\varphi+\frac{\partial w}{\partial x}\right)+\frac{\partial}{\partial x}\left(\Theta_{14}\left(\frac{\partial^2 w}{\partial x^2}\right)\right)$$
$$-\frac{\partial}{\partial x}\left(\Theta_{12}\left(\frac{\partial\varphi}{\partial x}+\frac{\partial^2 w}{\partial x^2}\right)\right)+\frac{1}{2}l^2\frac{\partial}{\partial x}\left(\Theta_{14}\left(\frac{\partial^2 w}{\partial x^2}\right)\right) \quad (10c)$$
$$-\frac{1}{4}l^2\frac{\partial}{\partial x}\left(\Theta_8\left(\frac{\partial\varphi}{\partial x}+\frac{\partial^2 w}{\partial x^2}\right)\right)=0$$

Also, boundary conditions are:

'$\delta u$'

$$\Theta_8\left(\frac{\partial u}{\partial x}\right)=0 \quad (11a)$$

'$\delta w$'

$$\Theta_{14}\left(\frac{\partial\varphi}{\partial x}+\frac{\partial^2 w}{\partial x^2}\right)+\frac{1}{2}\Theta_8\left(\varphi+\frac{\partial w}{\partial x}\right)$$
$$+\frac{1}{4}l^2\Theta_8\left(\varphi+\frac{\partial w}{\partial x}\right)+F\frac{\partial w}{\partial x}-l^2\Theta_{16}\left(\frac{\partial^2 w}{\partial x^2}\right) \quad (11b)$$
$$-\Theta_{12}\left(\frac{\partial\varphi}{\partial x}+\frac{\partial^2 w}{\partial x^2}\right)+l^2\Theta_{16}\left(\frac{1}{2}\frac{\partial\varphi}{\partial x}+\frac{\partial^2 w}{\partial x^2}\right)$$
$$-\frac{3}{8}l^2\Theta_8\left(\frac{\partial\varphi}{\partial x}+\frac{\partial^2 w}{\partial x^2}\right)=0$$

'$\delta\varphi$'

$$\Theta_{14}\frac{\partial\varphi}{\partial x}+\frac{1}{4}l^2\Theta_8\left(\frac{\partial\varphi}{\partial x}+\frac{\partial^2 w}{\partial x^2}\right)-\frac{1}{2}l^2\Theta_{16}\left(\frac{\partial^2 w}{\partial x^2}\right)=0 \quad (11c)$$

where

$$\{\Theta_8 \quad \Theta_{14} \quad \Theta_{16}\}=\iint\{E \quad Ez^2 \quad G\}(x,r)rdrd\theta \quad (12)$$

## 3. Solution methodology

The study uses the finite element method (FEM) to investigate the buckling behavior of a porosity-dependent, nonuniform functionally graded material tube, with a focus on material gradation and small-scale effects. This numerical method effectively addresses the challenges posed by nonuniform cross-sections and porosity distributions, making it appropriate for sports applications requiring lightweight structures with increased stability. The non-uniform FGM tube is discretized into Timoshenko beam elements, which account for transverse shear deformation and rotational inertia effects. The structure is divided into finite elements of variable lengths, allowing for precise modeling of nonuniform geometry and porosity effects. The material properties vary along the length of the tube and are computed at integration points within each element (Li *et al*. 2022, Zhang *et al*. 2024a). The displacement fields are approximated with interpolation functions (shape functions).

Lagrange interpolation functions are used for axial displacement ($u$), and Hermite polynomials for transverse displacement ($w$) and rotation ($\varphi$). The stiffness matrix ($K_e$) of each element is derived using the virtual work principle and expressed as:

$$[K_e]=\int_0^L B^T DBdx \quad (13a)$$

where 'B' and 'D' are the strain and elasticity matrix, respectively. Similarly, the mass matrix ($M_e$) of each element is given by:

$$[M_e]=\int_0^L \frac{\partial}{\partial x}\left(F\frac{\partial w}{\partial x}\right)dx \quad (13b)$$

The matrices are calculated numerically through Gaussian quadrature integration to accommodate nonuniform section properties. The element matrices are combined into global stiffness and mass matrices using the standard finite element assembly procedure. This step accounts for non-uniformity in geometry and material properties, resulting in an accurate representation of porosity-dependent mechanical behavior. Using Timoshenko beam theory, the displacement field within each element is approximated as:

$$u(x)=N_u(x)\{U\} \quad (14a)$$

$$w(x)=N_w(x)\{W\} \quad (14b)$$

$$u(\varphi)=N_\varphi(x)\{\Gamma\} \quad (14c)$$

where '$N_u$, $N_w$, and $N_\varphi$' are interpolation (shape) functions, and '$\{U\}$, $\{W\}$, and $\{\Upsilon\}$' are nodal displacement vectors. Where

$$N_u(x)=\left[1-\frac{x}{L_e}, \quad \frac{x}{L_e}\right] \quad (14d)$$

Hermite cubic polynomials ensure continuity in transverse displacement ($w$) and rotation ($\varphi$).

$$N_w(x)=N_\varphi(x)=\begin{bmatrix}1-3\frac{x^2}{{L_e}^2}+2\frac{x^3}{{L_e}^3}, x-2\frac{x^2}{L_e}+\frac{x^3}{{L_e}^2}, \\ 3\frac{x^2}{{L_e}^2}-2\frac{x^3}{{L_e}^3}, -\frac{x^2}{L_e}+\frac{x^3}{{L_e}^2}\end{bmatrix} \quad (14e)$$

The element matrices are assembled into global stiffness, mass, and geometric stiffness matrices:

$$[K_e]\{q\}=\lambda[M_e]\{q\} \quad (14f)$$

where '$\lambda$' and '$q$' are the buckling eigenvalue and buckling eigen vectors, respectively. The critical buckling loads are determined by solving the generalized eigenvalue problem:

$$det([K_e]-\lambda[M_e])=0 \quad (14g)$$

Table 1 Validation of calculated numerical buckling load ($F\,L^2/\iint Er^3\,sin^2(\theta)drd\theta$) for pinned tube versus the aspect ratio compared to other research results

| | ‘$\frac{L}{R_{initial}-R_{in}}=$ 10’ | ‘$\frac{L}{R_{initial}-R_{in}}=$ 20’ | ‘$\frac{L}{R_{initial}-R_{in}}=$ 100’ |
|---|---|---|---|
| Wang *et al*. (2024b), High-order tube theory | | | |
| | 9.609656938 | 9.787789586 | 9.87135321 |
| Zhang *et al*. (2023a), High-order tube theory | | | |
| | 9.610618 | 9.788279 | 9.86642 |
| Reddy (2007), first-order shear deformation beam theory | | | |
| | 9.6227 | 9.8067 | 9.8671 |
| Present study, first-order shear deformation beam theory | | | |
| | 9.62366227 | 9.79787397 | 9.86611329 |

Table 2 Comparison and validation of numerical buckling load ($F\,L^2/\iint Er^3\,sin^2(\theta)drd\theta$) of the current study via results of Xia *et al*. (2025) versus the different boundary conditions as well as different types of radius functions involving the uniform, linear, convex, and concave types of section

| Uniform | Concave | Linear | Convex |
|---|---|---|---|
| Clamped type of boundary conditions | | | |
| Xia *et al*. (2025), High-order tube theory | | | |
| 10.06538 | 6.850861 | 6.812317 | 6.833164 |
| Present study, first-order shear deformation beam theory | | | |
| 10.0955761 | 6.80290497 | 6.76394955 | 6.78601517 |
| Pinned type of boundary conditions | | | |
| Xia *et al*. (2025), High-order tube theory | | | |
| 2.516346 | 1.69825 | 1.747681 | 1.880133 |
| Present study, first-order shear deformation beam theory | | | |
| 2.52389504 | 1.68636225 | 1.73527246 | 1.86716008 |

The FEM formulation is implemented in MATLAB/ Python using the following steps:

• Mesh generation involves refining nonuniform elements to capture porosity effects.

• Matrix assembly is the process of calculating global stiffness, mass, and geometric stiffness matrices.

• Eigenvalue computation involves solving for critical buckling loads.

• Result Interpretation: Identifying the best designs for sports applications.

## 4. Presentation of numerical results

This section presents the numerical results of a finite element analysis that examined the effects of porosity, material gradation, and geometric nonuniformity on the buckling behavior of functionally graded microtubes. Critical trends in stability performance are identified by rigorously assessing key parameters such as the gradation index, porosity coefficient, and cross-sectional tapering. These findings are critical for developing lightweight, structurally resilient components in sports engineering. To ensure the accuracy and dependability of the results, the numerical findings are compared to established analytical solutions and previous studies on FGM beams. In addition to theoretical validation, the implications of these findings are investigated in practical applications such as bicycle frames, ski poles, and gymnastic vaulting poles, where an optimal balance of weight reduction and structural integrity is required. This analysis combines computational mechanics and practical sports engineering, providing critical insights for developing high-performance sports equipment.

To validate the accuracy of the proposed finite element framework, the numerical buckling loads obtained in this study were compared to previously published analytical and numerical results. These comparisons are summarized in Tables 1 and 2, which show strong agreement and confirm the current methodology's reliability.

Table 1 compares the dimensionless critical buckling load ( $F\,L^2/\iint Er^3\sin^2(\theta)drd\theta$ ) of a pinned FGM microtube across varying aspect ratios ($L/(R_{initial}-R_{in})$). The results are benchmarked against high-order tube theory solutions from Wang *et al*. (2024b) and Zhang *et al*. (2023a), as well as first-order shear deformation beam theory (FSDT) results from Reddy (2007). The present FSDT-based FEM results exhibit excellent agreement with all references, with relative errors of less than 0.15%, confirming the robustness of the formulation. For instance, at '$L/(R_{initial}-R_{in})=10$', the buckling load calculated in this study (9.6237) aligns closely with Reddy's FSDT solution (9.6227). Minor discrepancies at higher aspect ratios (e.g., 9.8661 vs. 9.8713 for '$L/(R_{initial}-R_{in})=100$' arise from differences in higher-order shear deformation assumptions but remain within acceptable tolerances.

Table 2 broadens the validation to include various boundary conditions and cross-sectional radius functions (uniform, concave, linear, convex). The findings are compared with those of Xia *et al*. (2025), who utilized high-order tube theory. For clamped boundary conditions, the FSDT-based buckling loads obtained in this study (e.g., 10.0956 for uniform sections) closely align with the high-order solutions provided by Xia *et al*. (10.0654), exhibiting deviations of less than 0.3%. A comparable agreement is noted for pinned boundaries, with the current results (e.g., 2.5239 for uniform sections) differing by less than 0.4% from the values reported by Xia *et al*. (2.5163). The concave and convex radius functions demonstrate slightly reduced buckling loads relative to uniform sections, indicating the sensitivity of stability to geometric nonuniformity. The current FEM model and reference studies consistently capture these trends, thereby validating the framework's capacity to manage complex geometries and boundary conditions.

The strong correlation of results in Tables 1 and 2 highlights the effectiveness of the proposed FEM method in forecasting the buckling behavior of nonuniform FGM microtubes. The observed minor deviations are ascribed to variations in theoretical assumptions, such as high-order versus first-order shear deformation, and numerical discretization strategies. The validations indicate that the existing methodology serves as a dependable instrument for assessing stability performance in sports engineering contexts, where accurate predictions of buckling resistance are essential for lightweight, high-strength designs.

This study investigates a functionally graded material composed of carbon fiber-reinforced polymer (CFRP) and aluminum alloy (Al 6061), which is widely regarded as the optimal combination for sporting applications. This FGM combines CFRP's high strength-to-weight ratio and stiffness with aluminum's ductility, toughness, and impact resistance. This combination is ideal for sports equipment such as bicycle frames, ski poles, and vaulting poles that need to be lightweight, strong, and long-lasting. The CFRP phase provides the required stiffness and load-bearing capacity, while the aluminum phase improves energy absorption and dynamic load resistance, ensuring performance and safety (Mallick 2007). The mechanical properties of these phases have been extensively studied in the literature. CFRP's elastic modulus ranges from 70 to 200 GPa, depending on fiber orientation and volume fraction, with a Poisson's ratio of 0.28 to 0.34 (Jones 1999). The elastic modulus of aluminum alloy (Al 6061) is 68.9 GPa, while the Poisson's ratio is 0.33 (Handbook-Committee 1990). CFRP-Al FGM is appropriate for sports engineering due to its properties, which enable the construction of lightweight structures with tailored stiffness and strength.

In this study, the dimensionless buckling load (Δ) is used to evaluate the stability of functionally graded microtubes. The parameter is defined as:

$$\Delta = F\frac{L^2}{\pi^2}\left(\iint E_{Al\ 6061} r^3 sin^2(\theta) dr d\theta\right)^{-1} \tag{15}$$

In this equation, '$F$' represents the applied axial load, '$L$' represents the microtube's length, '$E_{Al\ 6061}$' is the elastic modulus, '$r$' is the radial coordinate, and '$\theta$' is the circumferential angle. The denominator integral takes into account the material distribution and cross-sectional geometry of the microtubes. This dimensionless formulation allows for the comparison of buckling behaviors across different microtube configurations and material gradations by normalizing the critical buckling load against geometric and material parameters. Such normalization is required to understand how factors such as porosity, material gradation, and geometric nonuniformity affect the stability performance of functionally graded microtubes.

This section provides the numerical results of the buckling analysis for porosity-dependent, nonuniform, functionally graded microtubes and examines their implications for sports engineering applications. This research analyzes the primary factors affecting buckling loads, such as small-scale modified couple stress effects, material gradation, porosity, and cross-sectional shape. Specifications are critical for producing lightweight, high-performance sports equipment such as bicycle frames, ski poles, and vaulting poles.

Fig. 3 demonstrates the relationship between buckling load and the small-scale modified couple stress parameter for various cross-sectional geometries and boundary conditions.

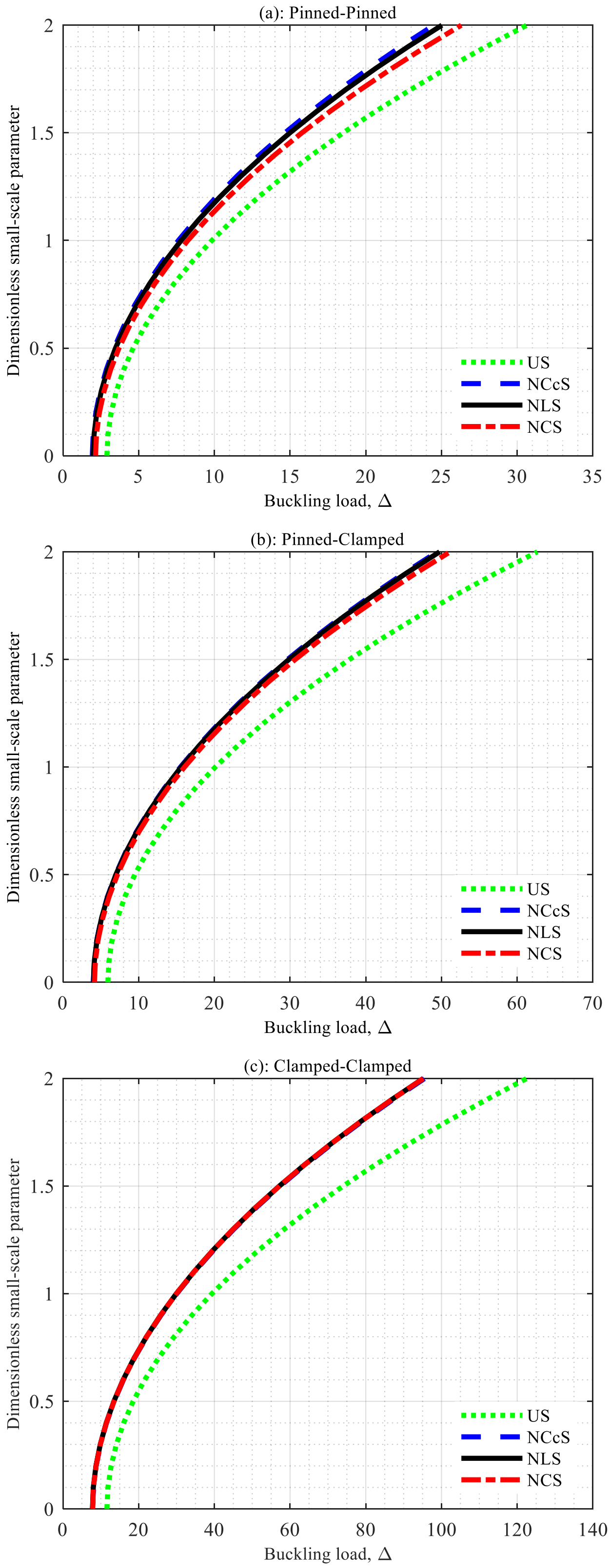


Fig. 3 Dimensionless buckling load (Δ) of microtube versus the small-scale modified couple stress parameter ($l^2/R_{initial}$) for different boundary conditions for both uniform section (US) and nonuniform sections involving the nonuniform linear section (NLS), nonuniform concave section (NCcS), and nonuniform convex section (NCS) types, $L = 20(R_{initial} - R_{in})$

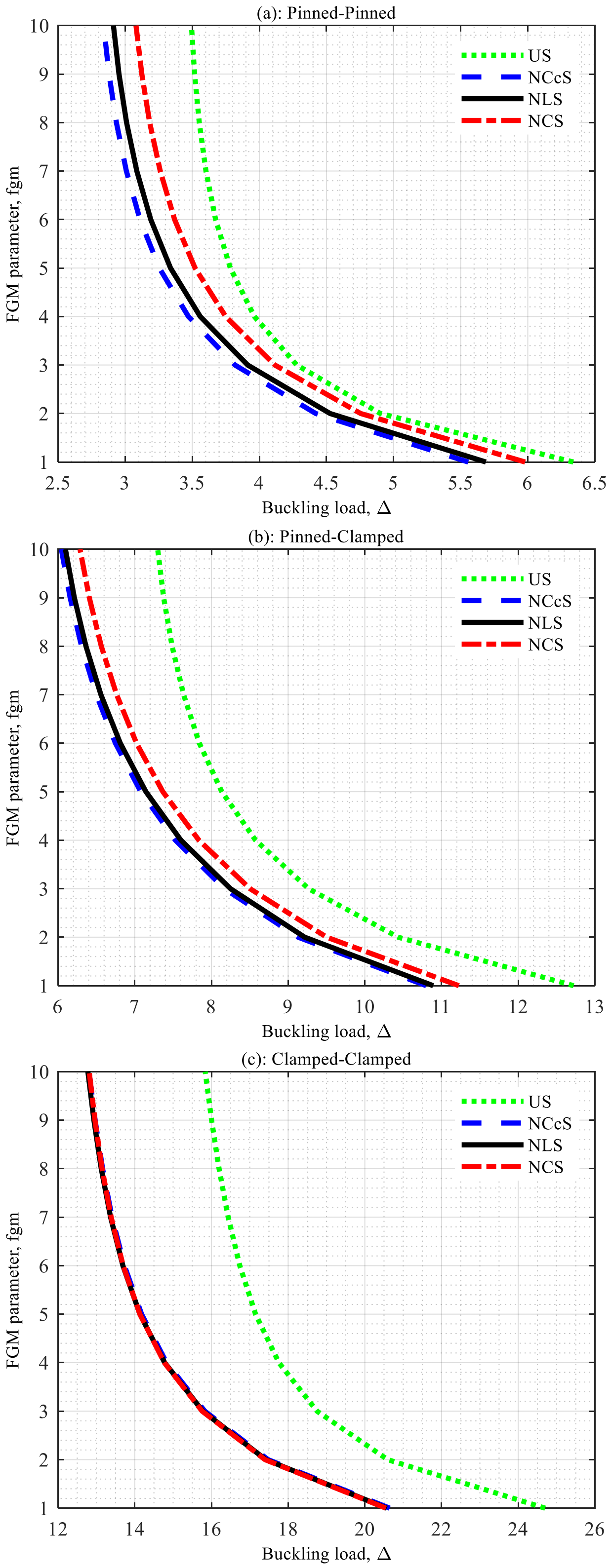


Fig. 4 Impact of FGM parameter (fgm), on numerical buckling load (Δ) of FG microtube, versus the different cross-section as well as different boundary conditions, $l^2 = R_{initial}$, $L = 20(R_{initial} - R_{in})$

The results indicate that an increase in the small-scale parameter ($l$) is associated with a rise in the buckling load, implying enhanced structural stability. Clamped arrangements produce the highest buckling loads by limiting rotational flexibility, whereas pinned configurations yield the lowest loads due to increased rotational compliance.

The results indicate that uniform sections exhibit better resistance to buckling than nonuniform sections. In the nonuniform category, convex profiles demonstrate superior performance to concave profiles due to enhanced stress distribution and stability. The findings possess considerable practical implications. Clamped connections and uniform cross-sections in vaulting poles and bicycle frames enhance load-bearing capacity. Intentionally integrating nonuniform shapes, such as convex tips on ski poles, enhances flexibility while preserving overall strength. The size-dependent parameter $l$ enhances deformation resistance via microstructural interactions. This is particularly advantageous for smaller athletic components. The results establish a foundation for optimizing material distribution and boundary constraints in sports equipment, enhancing performance and ensuring player safety.

Fig. 4 shows the numerical buckling load of microtubes made from functionally graded materials as a function of the FGM parameter ($fgm$). These results were obtained pinned, clamped, and mixed boundary conditions using the same cross-sectional geometries as in Figure 3. The analysis indicates that an increase in the FGM parameter results in a reduction of the buckling load. The observed behavior results from a reduction in the volume fraction of carbon fiber reinforced polymer (CFRP) in the composite material. The elastic modulus of CFRP is considerably more significant, with values ranging from 70 to 200 GPa, compared to aluminum alloys, which have an elastic modulus of approximately 68.9 GPa. Augmenting the FGM parameter reduces the composite's overall stiffness, resulting in a decrease in buckling resistance.

Fig. 3 depicts the effects of cross-sectional geometry and boundary conditions on buckling loads. These findings are directly applicable to the design of sports equipment, where strategic material gradation can be used to customize performance characteristics.

A CFRP-rich gradation ($fgm \approx 0$) in high-stress areas, such as the heads of tennis rackets or hockey sticks, improves stiffness and power transfer. In contrast, an aluminum-rich gradation ($fgm > 2$) in areas such as grips can improve vibration damping and user comfort by maintaining an optimal balance of rigidity and flexibility.

Fig. 5 illustrates how the porosity parameter (β) affects numerical buckling load across various cross-sectional geometries while accounting for different material distributions: pure CFRP, pure aluminum alloy, and their combination as a functionally graded material. The results indicate that buckling load decreases linearly as porosity increases. CFRP exhibits the highest buckling load among the materials, succeeded by FGM composite, whereas aluminum alloy demonstrates the lowest buckling load. This hierarchy reflects the inherent stiffness of the materials, demonstrating that CFRP possesses greater stiffness than aluminum alloys. Comprehending the significance of porosity in sports applications is essential for enhancing the strength-to-weight ratio of equipment, ensuring durability, and

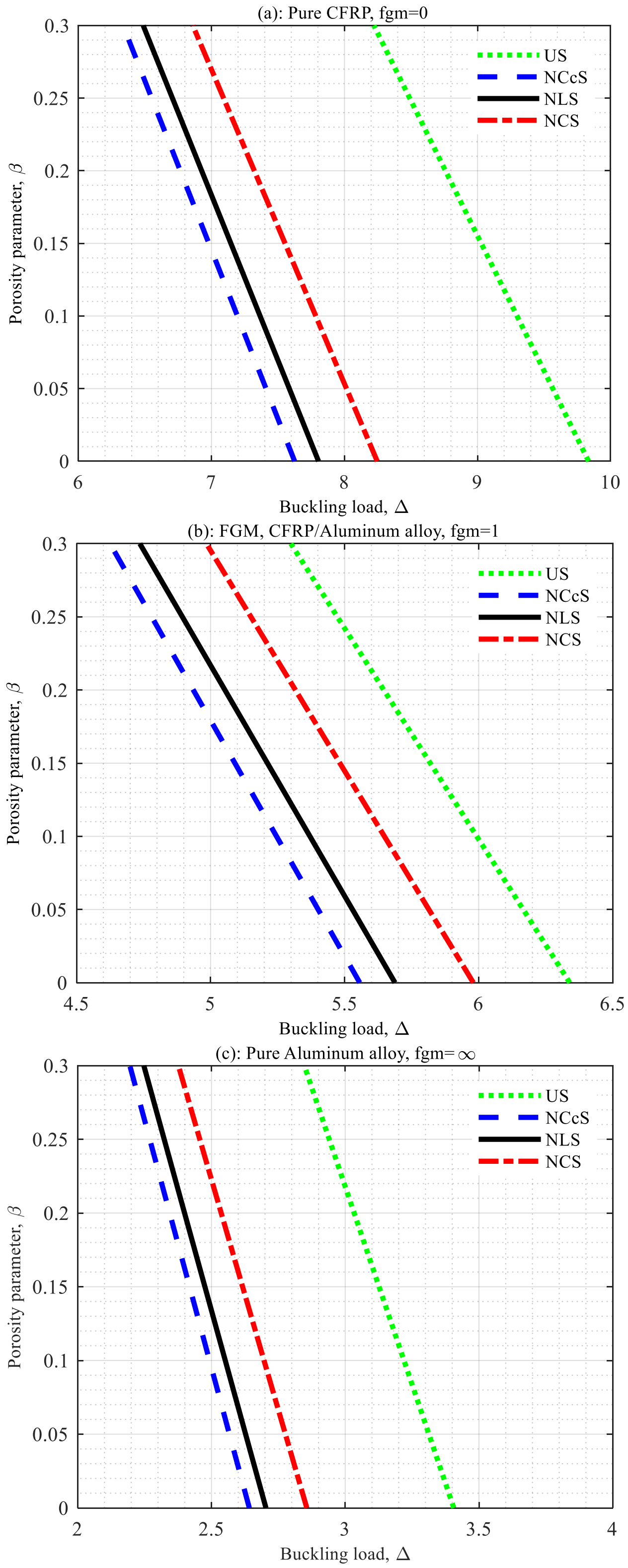


Fig. 5 Impact of porosity parameter (β) on the numerical buckling load (Δ) of pinned microtube versus the different cross-sections for pure Aluminum alloy, pure CFRP, and their composition (FGM CFRP/Aluminum alloy), $l^2 = R_{initial}$, $L = 20(R_{initial} - R_{in})$

optimizing performance efficiency.

The numerical results indicate that small-scale effects, material gradation, geometric nonuniformity, and porosity all have a significant impact on the buckling behavior of functionally graded microtubes. These findings have important implications for the design and development of sports equipment, allowing for the creation of lightweight and mechanically resilient structures.

Porosity creates localized weaknesses, reducing the effective load-bearing area and stiffness. CFRP has significantly better mechanical properties than aluminum ($E_{CFRP} \gg E_{Al}$), making it less vulnerable to the effects of porosity. Maintaining structural integrity in protective gear, such as helmets and rowing oars, requires minimizing porosity ($\beta < 0.2$). CFRP-aluminum functionally graded materials combine CFRP stiffness with aluminum's energy absorption properties, resulting in improved safety and performance.

## 5. Conclusions

This research examined the buckling characteristics of porosity-dependent, nonuniform functionally graded material microtubes utilizing a finite element approach grounded in Timoshenko beam theory and modified couple stress theory. The analysis examined the impact of critical parameters size-dependent mechanics, material gradation, porosity, and cross-sectional geometry on the stability performance of microscale structures. The results offer essential insights for enhancing the design of lightweight, high-performance sports equipment, where structural integrity and weight optimization are crucial.

Key conclusions include:

• Size-Dependent Effects: The buckling load increases with the small-scale parameter ($l$), emphasizing the significance of microstructural interactions in improving the stability of small-scale components. This effect is especially important for sports equipment such as bicycle chain stays and gymnastic grips, where microscale geometry and material behavior dominate performance.

• Boundary Conditions: Clamped configurations have much higher buckling resistance than pinned or pinned-clamped conditions. This emphasizes the role of constrained joints in sports equipment, such as vaulting poles and bicycle frames, in increasing load-bearing capacity.

• Cross-Sectional Geometry: Uniform cross-sections have higher buckling resistance because of their symmetric stress distribution. Nonuniform profiles, such as convex sections, provide an excellent balance of flexibility and strength, making them ideal for adaptive designs like ski poles and archery bows.

• Material Gradation: Buckling resistance is inversely related to the FGM parameter, with CFRP-rich compositions (fgm≈0) demonstrating the greatest stability. Material gradation facilitates enhanced designs, including rigid CFRP areas in tennis racket heads and aluminum-rich grips for vibration attenuation.

• Porosity Effects: Porosity reduces buckling loads by introducing localized vulnerabilities. Reducing porosity (β<0.3) in critical areas of protective equipment, like helmets or rowing oars, preserves structural integrity and lightweight benefits.

The results indicate that the integration of advanced materials science and computational mechanics has the potential to transform sports engineering. Engineers can create equipment that integrates lightweight characteristics with remarkable stability by optimizing functionally graded materials gradation, regulating porosity, and selecting suitable cross-sectional geometries. CFRP-aluminum FGMs with clamped uniform sections are optimal for high-stress applications such as bicycle frames, while nonuniform convex profiles with regulated porosity enhance flexibility in ski poles without compromising durability.

This study combines theoretical mechanics with real-world sports applications, providing a solid foundation for developing next-generation athletic equipment. Future research could look into dynamic loading conditions, fatigue resistance, and experimental validation to help refine these models. Using the findings of this study, sports engineers can push the boundaries of performance, safety, and innovation, ultimately improving athletic achievement and equipment reliability.

## Acknowledgement

This work was supported by

1. Research Project on Higher Education Teaching Reform in Shaanxi Province in 2023. Project Number: 23ZY016.

Topic: Exploration and Practice of Dynamic Layered Teaching Mode in College Physical Education Teaching Based on the Concept of “Three pronged Education”.

2. Tianshui Normal University Research and Innovation Fund Special Project. Project Number: CXJ2023-09.

Topic: Research on the Innovative Path of Tennis Culture Construction and Communication in Ordinary Colleges and Universities.

## References

Afshari Behzad, M., Mirjavadi Seyed, S. and Barati Mohammad, R. (2022), “Investigating nonlinear static behavior of hyper-elastic plates using three-parameter hyperelastic model”, *Adv. Concr. Constr.*, **13**(5), 377-384. https://doi.org/10.12989/ACC.2022.13.5.377.

Chen, F., Chen, J., Duan, R., Habibi, M. and Khadimallah, M.A. (2022), “Investigation on dynamic stability and aeroelastic characteristics of composite curved pipes with any yawed angle”, *Compos. Struct.*, **284**, 115195. https://doi.org/10.1016/j.compstruct.2022.115195.

Dai, Z., Jiang, Z., Zhang, L. and Habibi, M. (2021), “Frequency characteristics and sensitivity analysis of a size-dependent laminated nanoshell”, *Adv. Nano Res.*, **10**(2), 175-189. https://doi.org/10.12989/anr.2021.10.2.175.

El-Galy, I.M., Saleh, B.I. and Ahmed, M.H. (2019), “Functionally graded materials classifications and development trends from industrial point of view”, *SN Appl. Sci.*, **1**(11), 1378. https://doi.org/10.1007/s42452-019-1413-4.

Gao, Z., Xu, N., Zong, G., Wang, H., Niu, B. and Zhao, X. (2025), “Fuzzy weight-based secure formation control for two-order heterogeneous multi-agent systems via reinforcement learning”, *Inform. Sci.*, **698** 121782. https://doi.org/10.1016/j.ins.2024.121782.

Godat, A., Legeron, F. and Bazonga, D. (2012), “Stability investigation of local buckling behavior of tubular polygon columns under concentric compression”, *Thin Walled Struct.*, **53**, 131-140. https://doi.org/10.1016/j.tws.2011.12.013.

Gu, J., Qin, Y., Gao, H., Yan, Y., Yang, J., Yang, K. and Mi, C. (2022), “Nonlinear buckling analysis of tower crane structure based on movable boundaries”, *Adv. Mech. Eng.*, **14**(11), 16878132221138308. https://doi.org/10.1177/16878132221138308.

Guo, Y., Maalla, A., Habibi, M. and moradi, Z. (2024), “Electroelastic wave dispersion in the rotary piezoelectric NEMS sensors/actuators via nonlocal strain gradient theory”, *Mech. Syst. Signal Pr.*, **216**, 111453. https://doi.org/10.1016/j.ymssp.2024.111453.

Handbook-Committee, A. (1990), “Properties and selection: nonferrous alloys and special-purpose materials”. https://doi.org/10.31399/asm.hb.v02.9781627081627.

He, L., Habibi, M. and Khorami, M. (2024), “Semi-analytical stability behavior of composite concrete structures via modified non-classical theories”, *Adv. Concr. Constr.*, **17**(4), 187. https://doi.org/10.12989/acc.2024.17.4.187.

He, X., Zhang, K., Jiang, S., Jiang, Z., Wang, X., Jiang, W., Li, J., Wu, Y., Gao, Z., Tang, T., Yang, C., Yuan, X., Han, F., Wang, Z. and Ye, L. (2025), “Influencing factors and quantitative prediction of gas content of deep marine shale in Luzhou block”, *Sci. Rep.*, **15**(1), 1896. https://insu.hal.science/insu-02453795/10.1038/s41598-025-86095-8.

Huo, J., Zhang, G., Ghabussi, A. and Habibi, M. (2021), “Bending analysis of FG-GPLRC axisymmetric circular/annular sector plates by considering elastic foundation and horizontal friction force using 3D-poroelasticity theory”, *Compos. Struct.*, **276** 114438. https://doi.org/10.1016/j.compstruct.2021.114438.

Jia, S., Niu, X., Jia, F. and Mahmoudi, T. (2023), “Advantages and disadvantages of renewable energy-oil-environmental pollution-from the point of view of nanoscience”, *Adv. Concr. Constr.*, **16**(1), 69-78. https://doi.org/10.12989/acc.2023.16.1.069.

Jining, L., Yunzhu, A., Habibi, M., Aihui, W., Ming, M., Guoyin, S. and Lingling, S. (2025), “A hybrid intelligent model for deformation/strain/stress analyses of sandwich double curved piezoelectric shells”, *Int. J. Struct. Stabil. Dyn.*, Accepted. https://doi.org/10.1142/S021945542650166X.

Jones, R.M. (1999), *Mechanics of Composite Materials*, CRC Press, Boca Raton. https://doi.org/10.1201/9781498711067.

Kazemi, M., Nabavi, S., Gratuze, M. and Nabki, F. (2023), “Anchor loss reduction in micro-electro mechanical systems flexural beam resonators using trench hole array reflectors”, *Micromachines*, 14(11), 2036. https://doi.org/10.3390/mi14112036.

Kazemi, M., Nabavi, S., Gratuze, M. and Nabki, F. (2024), “Frequency selection in a MEMS flexural beam resonator by electrostatic actuation”, *J. Microelectromech. Syst.*, **33**(1), 66-77. https://doi.org/10.1109/JMEMS.2023.3331701.

Leoni, F., Dal Fabbro, P., Rosso, S., Grigolato, L., Meneghello, R., Concheri, G. and Savio, G. (2023), “Functionally graded additive manufacturing: bridging the gap between design and material extrusion”, *Appl. Sci.*, **13**(3). https://doi.org/10.3390/app13031467.

Li, X., Luo, L., Habibi, M. and Wang, L. (2025a), “Extending a higher-order foldability constitutive model for dynamic response analysis of 3D-reinforced shell of deformable”, *Acta Mech.*, 1-25. https://doi.org/10.1007/s00707-024-04216-2.

Li, Y., Habibi, M. and Bagheri, M. (2024), “AI-driven prediction of linear and nonlinear buckling in nonuniform functionally graded micro-tubes for sports equipment in sports training”, *Adv. Nano Res.*, **17**(6), 559. https://doi.org/10.12989/anr.2024.17.6.559.

Li, Y., Li, S., Guo, K., Fang, X. and Habibi, M. (2022), “On the modeling of bending responses of graphene-reinforced higher order annular plate via two-dimensional continuum mechanics approach", *Eng. Comput.*, **38**(1), 703-724. https://doi.org/10.1007/s00366-020-01166-w.

Li, Y., Weng, X., Hu, D., Tan, Z., Qi, K. and Liu, J. (2025b), "Data-driven deep-learning model for predicting jacking force of rectangular pipe jacking tunnel", *J. Comput. Civil Eng.*, **39**(3), 04025017. https://doi.org/10.1061/JCCEE5.CPENG-6167.

Liang, Z., Zhao, Y., Yu, H., Habibi, M. and Mahmoudi, T. (2024), "Artificial neural networks coupled with numerical approach for the stability prediction of non-uniform functionally graded microscale cylindrical structures", *Structures*, **60**, 105826. https://doi.org/10.1016/j.istruc.2023.105826.

Lin, H. and Qiyuan, D. (2023), "Construction of sports engineering structures with high resistance to improve the quality of sports training", *Struct. Eng. Mech.*, **86**(2), 211-220. https://doi.org/10.12989/sem.2023.86.2.211.

Liu, C., Chen, M., Habibi, M. and Chen, X. (2025), "Effect of micro-scale parameter and thermal loads on the stress/strain/ displacement distribution of micro-plate", *J. Vib. Eng. Technol.*, **13**(1), 130. https://doi.org/10.1007/s42417-024-01597-5.

Mallick, P.K. (2007), *Fiber-Reinforced Composites: Materials, Manufacturing, and Design*, CRC Press.

Man, Y., Habibi, M. and Maleki, B. (2024), "Biodiesel synthesis from waste coconut scum oil utilizing SnFe2O4/cigarette butt-derived biochar as a magnetic nanocatalyst: Optimization, kinetic and thermodynamic study", *Chem. Eng. Res. Des.*, **210**, 311-327. https://doi.org/10.1016/j.cherd.2024.08.033.

Mirjavadi, S.S., Afshari, B.M., Barati, M.R. and Hamouda, A.M.S. (2020a), "Transient response of porous inhomogeneous nano-beams due to various impulsive loads based on nonlocal strain gradient elasticity", *Int. J. Mech. Mater. Des.*, **16**(1), 57-68. https://doi.org/10.1007/s10999-019-09452-2.

Mirjavadi, S.S., Forsat, M., Badnava, S. and Barati, M.R. (2020b), "Analyzing nonlocal nonlinear vibrations of two-phase geometrically imperfect piezo-magnetic beams considering piezoelectric reinforcement scheme", *J. Strain Anal. Eng. Des.*, **55**(7-8), 258-270. https://doi.org/10.1177/0309324720917285.

Mirjavadi, S.S., Forsat, M., Badnava, S., Barati, M.R. and Hamouda, A.M.S. (2020c), "Nonlinear dynamic characteristics of nonlocal multi-phase magneto-electro-elastic nano-tubes with different piezoelectric constituents", *Appl. Phys. A.* **126**(8), 605. https://doi.org/10.1007/s00339-020-03743-8.

Mirjavadi, S.S., Forsat, M., Barati, M.R. and Hamouda, A. (2020d), "Investigating nonlinear vibrations of multi-scale truncated conical shell segments with carbon nanotube/ fiberglass reinforcement using a higher order conical shell theory", *J. Strain Anal. Eng. Des.*, **56**(3), 181-192. https://doi.org/10.1177/0309324720939811.

Mirjavadi, S.S., Forsat, M., Barati, M.R. and Hamouda, A.M.S. (2022a), "Analysis of nonlinear vibrations of CNT- /fiberglass-reinforced multi-scale truncated conical shell segments", *Mech. Based Des. Struct.*, **50**(6), 2067-2083. https://doi.org/10.1080/15397734.2020.1768866.

Mirjavadi, S.S., Forsat, M., Barati, M.R. and Hamouda, A.M.S. (2022b), "Geometrically nonlinear vibration analysis of eccentrically stiffened porous functionally graded annular spherical shell segments", *Mech. Based Des. Struct.*, **50**(6), 2206-2220. https://doi.org/10.1080/15397734.2020.1771729.

Mirjavadi, S.S., Forsat, M., Barati, M.R. and Hamouda, A.M.S. (2022c), "Nonlinear vibrations of variable thickness curved panels made of multi-scale epoxy/fiberglass/CNT material using Jacobi elliptic functions", *Mech. Based Des. Struct.*, **50**(7), 2333-2349. https://doi.org/10.1080/15397734.2020.1777156.

Mirjavadi, S.S., Khan, I., Forsat, M., Barati, M.R. and Hamouda, A.M.S. (2023), "Analyzing nonlinear vibration of metal foam stiffened toroidal convex/concave shell segments considering porosity distribution", *Mech. Based Des. Struct.*, **51**(1), 310-326. https://doi.org/10.1080/15397734.2020.1841654.

Mirjavadi, S.S., Yahya, Y.Z., Forsat, M., Khan, I., Hamouda, A.M.S. and Barati, M.R. (2020e), "Magneto-electric effects on nonlocal nonlinear dynamic characteristics of imperfect multi-phase magneto-electro-elastic beams", *J. Magn. Magn. Mater.*, **503** 166649. https://doi.org/10.1016/j.jmmm.2020.166649.

Mousavi, S.M., Shafiei, N. and Dadvand, A. (2017), "Numerical simulation of subsonic turbulent flow over NACA0012 airfoil: evaluation of turbulence models", *Sigma J. Eng. Natural Sci.*, **35**(1), 133-155.

Nayak, P. and Armani, A. (2022), "Optimal design of functionally graded parts", *Metals*, **12**(8), 1335. https://doi.org/10.3390/met12081335.

Omidi, S., Oskooee, M.B. and Shafiei, N. (2013), "Finite element analysis of an ultra-fine grained Titanium dental implant covered by different thicknesses of hydroxyapatite layer", *Indian J. Dent.*, **4**(1), 1-4. https://doi.org/10.1016/j.ijd.2012.10.002.

Panchal, Y. and Ponappa, K. (2022), "Functionally graded materials: A review of computational materials science algorithms, production techniques, and their biomedical applications", *Proceedings of the Institution of Mechanical Engineers, Part C: Journal of Mechanical Engineering Science*. **236**(22), 10969-10986. https://doi.org/10.1177/09544062221109261.

Partskhaladze, G., Mshvenieradze, I., Medzmariashvili, E., Chavleshvili, G., Yepes, V. and Alcala, J. (2019), "Buckling analysis and stability of compressed low-carbon steel rods in the elastoplastic region of materials", *Adv. Civil Eng.*, **2019**(1), 7601260. https://doi.org/10.1155/2019/7601260.

Qi, L., Wang, Z., Sun, Y., Khorami, M., Mahmoudi, T. and Wu, H. (2024), "Modified couple stress and artificial intelligence examination of nonlinear buckling in porous variable thickness cylinder micro sport structures", *Mech. Adv. Mater. Struct.*, 1-19. https://doi.org/10.1080/15376494.2024.2316795.

Reddy, J.N. (2007), "Nonlocal theories for bending, buckling and vibration of beams", *Int. J. Eng. Sci.*, **45**(2), 288-307. https://doi.org/10.1016/j.ijengsci.2007.04.004.

Saad, A.R. (2022), "A review on functionally graded materials and their applications in the field of prosthetics", *ERJ. Eng. Res. J.*, **45**(4), 553-560. https://doi.org/10.21608/erjm.2022.144631.1186.

Shahabinejad, E., Shafiei, N. and Ghadiri, M. (2018), "Influence of temperature change on modal analysis of rotary functionally graded nano-beam in thermal environment", *J. Solid Mech.*, **10**(4), 779-803. https://jsm.arak.iau.ir/article_545719.html.

Shi, X., Li, J. and Habibi, M. (2022), "On the statics and dynamics of an electro-thermo-mechanically porous GPLRC nanoshell conveying fluid flow", *Mech. Based Des. Struct.*, **50**(6), 2147-2183. https://doi.org/10.1080/15397734.2020.1772088.

Song, G., Zou, Y., Nie, Y., Habibi, M., Albaijan, I. and Toghroli, E. (2024), "Application of Hashin–Shtrikman bounds homogenization model for frequency analysis of imperfect FG bio-composite plates", *J. Mech. Behav. Biomed. Mater.*, **151**, 106321. https://doi.org/10.1016/j.jmbbm.2023.106321.

Wang, C., Habibi, M. and Mahmoudi, T. (2024a), "Stability analysis of the nonuniform functionally graded cylindrical small-scale beam structures: Application in sport structures", *Steel Compos. Struct.*, **52**(1), 15-29. https://doi.org/10.12989/scs.2024.52.1.015.

Wang, C., Habibi, M. and Mahmoudi, T. (2024b), "Stability analysis of the nonuniform functionally graded cylindrical small-scale beam structures: Application in sport structures", *Steel Compos. Struct.*, **52**(1), 15-29. https://doi.org/10.12989/scs.2024.52.1.015.

Wang, D., Bai, Y., Habibi, M. and Mahmoudi, T. (2024c), "Stability behaviors and governing equations of the volleyball game ball via GDQ and analytical methods", *Adv. Concr. Constr.*, **18**(6), 379-388. https://doi.org/10.12989/acc.2024.18.6.379.

Wang, D., Bai, Y., Habibi, M. and Mahmoudi, T. (2024d), "Stability behaviors and governing equations of the volleyball game ball via GDQ and analytical methods", *Adv. Concr. Constr.*, **18**(6), 379. https://doi.org/10.12989/acc.2024.18.6.379.

Wang, D., Feng, B., Liu, X., Habibi, M. and Mahmoudi, T. (2025a), "Nanoparticle-infused oils for improved lubrication and wear resistance in internal combustion engines: Exploring nanoscience applications in automotive parts", *Adv. Nano Res.*, **18**(1), 1-10. https://doi.org/10.12989/anr.2025.18.1.001.

Wang, D., Feng, B., Liu, X., Habibi, M. and Mahmoudi, T. (2025b), "Nanoparticle-infused oils for improved lubrication and wear resistance in internal combustion engines: Exploring nanoscience applications in automotive parts", *Adv. Nano Res.*, **18**(1), 1. https://doi.org/10.12989/anr.2025.18.1.001_

Wang, F., Gao, S., Habibi, M. and Luo, Z. (2024e), "Energy absorption of vibrating sport equipment used for testing athlete performance", *Adv. Nano Res.*, **17**(5), 421-434. https://doi.org/10.12989/anr.2024.17.5.421.

Wang, G., Sun, L. and Zhang, C. (2024f), "The effect of polyvinylpyrrolidone modified nano-polymers on rheological properties of silicon-based shear thickening fluid", *Phys. Fl.*, **36**(7), 073108. https://doi.org/10.1063/5.0213620.

Wang, N., Zhang, T., Yang, J., Habibi, M. and Feng, J. (2024g), "Electro-magneto-mechanical critical load analysis of piezo-electric/piezomagnetic sport force plates used for testing athlete performance", *Mech. Adv. Mater. Struct.*, 1-15. https://doi.org/10.1080/15376494.2024.2414944.

Wang, P., Gao, Z., Pan, F., Moradi, Z., Mahmoudi, T. and Khadimallah, M.A. (2022), "A couple of GDQM and iteration techniques for the linear and nonlinear buckling of bi-directional functionally graded nanotubes based on the nonlocal strain gradient theory and high-order beam theory", *Eng. Anal. Bound. Elem.*, **143**, 124-136. https://doi.org/10.1016/j.enganabound.2022.06.007.

Wang, T., Karimi, H.R., Wang, H., Xu, N., Li, L. and Zhao, X. (2025c), "A reinforcement learning methodology to hierarchical sliding-mode surface control of nonlinear systems via a dynamic event-triggered mechanism", *Asian J. Control*, **n/a**(n/a). https://doi.org/10.1002/asjc.3569.

Wang, W., Zhang, J., Habibi, M. and Albaijan, I. (2024h), "Stretchable-thickness model for dynamic responses of graphene origami reinforced badminton sport plate", *Mech. Adv. Mater. Struct.*, 1-13. https://doi.org/10.1080/15376494.2024.2373976.

Wang, Z., Yuan, Y., Zhang, S., Lin, Y. and Tan, J. (2024i), "A multi-state fusion informer integrating transfer learning for metal tube bending early wrinkling prediction", *Appl. Soft Comput.*, **151**, 110991. https://doi.org/10.1016/j.asoc.2023.110991.

Wei, F., Xu, N., Huang, S. and Cao, Y. (2024), "Disturbance observer–based adaptive neural finite-time control for nonstrict-feedback nonlinear systems with input delay", *Transactions of the Institute of Measurement and Control*. 01423312241261084. https://insu.hal.science/insu-02453795/10.1177/01423312241261084.

Wu, Y., Liang, H., Zhao, N. and Niu, B. (2024), "Low-computation-based adaptive self-triggered bipartite consensus control for nonlinear multiagent systems subject to sensor faults", *IEEE T Control Netw. Syst.*, **11**(4), 2114-2125.

Xia, L., Habibi, M. and Li, Q. (2025), "Computational stability analysis of sport structures: Importance of MEMS for testing athlete performance", *Steel Compos. Struct.*, **54**(1), 53. https://doi.org/10.12989/scs.2025.54.1.053.

Xiao, H., Habibi, M. and Habibi, M. (2024), "Bulk wave propagation analysis of imperfect FG bio-composite beams resting on variable elastic medium", *Mater. Today Commun.*, **39**, 108524. https://doi.org/10.1016/j.mtcomm.2024.108524.

Xue, L., Habibi, M. and Ou, C. (2024), "Stability and instability in responses of a concrete disk with non-classical boundary conditions", *Adv. Concr. Constr.*, **18**(5), 355. https://doi.org/10.12989/acc.2024.18.5.355.

Yan, C., Zhang, T., Zheng, T. and Mahmoudi, T. (2024), "Stability characteristic of bi-directional FG nano cylindrical imperfect composite: Improving the performance of sports bikes using carbon nanotubes", *Steel Compos. Struct.*, **50**(4), 459-474. https://doi.org/10.12989/scs.2024.50.4.459.

Yin, J., Zou, Y., Li, J., Zhang, W., Li, X. and Habibi, M. (2024), "Dynamic stability and frequency responses of the tilted curved nanopipes in a supersonic airflow via 2D hybrid nonlocal strain gradient theory", *Eng. Struct.*, **301**, 117240. https://doi.org/10.1016/j.engstruct.2023.117240.

Yu, C., Lin, P., Wu, Z., Habibi, M. and Zhang, W. (2024), "Multi-load effect on the deformation analysis of composite nano reinforced origami sandwich panel", *Mech. Adv. Mater. Struct.*, 1-19. https://doi.org/10.1080/15376494.2024.2367015.

Zhang, C., Liu, D., Zhang, X., Spencer, C., Tang, M., Zeng, J., Jiang, S., Jolivet, M. and Kong, X. (2020), "Hafnium isotopic disequilibrium during sediment melting and assimilation", *Geochem. Perspect. Lett.*, **12**, 34-39. https://doi.org/10.7185/geochemlet.2001.

Zhang, D., Huang, X., Wang, T., Habibi, M., Albaijan, I. and Toghroli, E. (2024a), "Dynamic stability improvement in spinning FG-piezo cylindrical structure using PSO-ANN and firefly optimization algorithm", *Mater. Sci. Eng. B*, **302**, 117210. https://doi.org/10.1016/j.mseb.2024.117210.

Zhang, H., Habibi, M. and Zou, Y. (2024b), "Static analysis of foldable pressurized and thermally loaded cylindrical shell as an expander in sport equipment reinforced by G-Ori nanofillers", *Mech. Adv. Mater. Struct.*, 1-13. https://doi.org/10.1080/15376494.2024.2412307.

Zhang, L., Chen, Z., Habibi, M., Ghabussi, A. and Alyousef, R. (2021), "Low-velocity impact, resonance, and frequency responses of FG-GPLRC viscoelastic doubly curved panel", *Compos. Struct.*, **269**, 114000. https://doi.org/10.1016/j.compstruct.2021.114000.

Zhang, P., Song, J. and Mahmoudi, T. (2023a), "Simulation and modeling for stability analysis of functionally graded non-uniform pipes with porosity-dependent properties", *Steel Compos. Struct.*, **48**(2), 235-250. https://doi.org/10.12989/scs.2023.48.2.235.

Zhang, Q., Xie, M., Zhou, D., Habibi, M. and Khorami, M. (2024c), "Bending responses of graphene nanoplatelets reinforced sandwich cylindrical micro panel with piezoelectric layers", *Mech. Adv. Mater. Struct.*, 1-16. https://doi.org/10.1080/15376494.2024.2385008.

Zhang, X., Li, J., Cui, Y., Habibi, M., Ali, H.E., Albaijan, I. and Mahmoudi, T. (2023b), "Static analysis of 2D-FG nonlocal porous tube using gradient strain theory and based on the first and higher-order beam theory", *Steel Compos. Struct.*, **49**(3), 293-306. https://doi.org/10.12989/scs.2023.49.3.293.

Zhang, Z., Du, J. and Mahmoudi, T. (2023c), "Green synthesis of silver nanoparticles to the microbiological corrosion deterrence of oil and gas pipelines buried in the soil", *Adv. Nano Res.*, **15**(4), 355-366. https://doi.org/10.12989/anr.2023.15.4.355.

Zhao, J., Wan, L., Habibi, M. and Brahmia, A. (2024), "An adaptive neuro-fuzzy approach using IoT data in predicting springback in ultra-thin stainless steel sheets with consideration of grain size", *Adv. Nano Res.*, **17**(2), 109. https://doi.org/10.12989/.2024.17.2.109.

Zhao, J., Xu, N., Niu, B., Zhao, X. and Alorfix, A.S. (2025), "Dynamic event-triggered optimal control for stochastic interconnected nonlinear systems with matched disturbances via adaptive dynamic programming", *J. Franklin Inst.*, **362**(2), 107360. https://doi.org/10.1016/j.jfranklin.2024.107360.

Zhiqiang, S., Aiyun, L., Daichang, Z., Shuangjun, L., Habibi, M., Xiaoling, F. and Albaijan, I. (2024), "Application of a folded nanostructure reinforcement for the pole vault curved shell", *Mech. Adv. Mater. Struct.*, 1-15. https://doi.org/10.1080/15376494.2024.2375368.

Zhou, W., Huang, Y., Wu, Z., Habibi, M., Habibi, M. and Marzouki, R. (2025), "Influence of agglomeration and waviness phenomena on torsional oscillation of MWCNTs-reinforced composite rods", *Int. J. Solids Struct.*, **306**, 113127. https://doi.org/10.1016/j.ijsolstr.2024.113127.

Zhu, J., Wang, Y., An, N., Habibi, M. and Wang, H. (2024a), "Application of G-Ori metamaterials as sports equipment baseball bat in an electro-magneto-elastic sandwich composite beam", *Mech. Adv. Mater. Struct.*, 1-20. https://doi.org/10.1080/15376494.2024.2414198.

Zhu, K., Ma, W., Dong, J., Chen, M., Habibi, M. and Albaijan, I. (2024b), "On the dispersion of bulk wave in hygrothermally affected poroelastic gymnastics beams based on refined higher-order shear deformation theory during athlete training", *Mech. Adv. Mater. Struct.*, 1-10. https://doi.org/10.1080/15376494.2024.2428830.

Zisong, Z. and Habibi, M. (2024), "AI-assisted prediction of St14 steel sheets formability: Neural-fuzzy systems and crystal plasticity assessments", *Structures*, **65**, 106633. https://doi.org/10.1016/j.istruc.2024.106633.

*JL*